Forward Flight Control Analysis of Bioinspired Flapping-Wing Micro Air Vehicle

Jong-Wan Lee, Jong-Seob Han, and Jae-Hung Han*
Korea Advanced Institute of Science and Technology, 291 Daehak-ro, Yuseong-gu, Daejeon, Republic of Korea

ABSTRACT

The forward flight control of FWMAV is studied at varying reference flight speeds. The semi-empirical quasi-steady aerodynamic model including effects of advance ratio is used to calculate the aerodynamic load on wings and control gain matrices are obtained using LQR method.

1 INTRODUCTION

To utilize the agility of flapping-wing micro air vehicle (FWMAV), many studies on the dynamic characteristic of flapping-wing MAV have been conducted. However, it is difficult to organize the control system for FWMAV under various flight conditions because of the high non-linearity and instability of FWMAV itself. Moreover, the linearization method, which has been widely used in the previous control studies of FWMAV, is valid only around the equilibrium points. It means that the controller obtained by using the linearized system equation around a specific equilibrium point may not properly work at other flight conditions. The quasi-steady aerodynamic model, which is easily applicable to dynamic analysis of FWMAV, needs to be revised in case of forward flights because the forward flight speed affects the stability of Leading-Edge Vortex (LEV) on the wing. There could be some error between the real aerodynamic loads and the results of the conventional quasi-steady aerodynamic model when FWMAV moves in forward direction. This study uses a semi-empirical quasi-steady model which is more accurate in forward flight than conventional quasi-steady model.

This study investigates the forward flight control of FWMAV at varying reference flight speeds.

2 MATERIALS AND METHOD

2.1 System modelling and coordinate definition

The FWMAV model consists of the body and one pair of wings. The morphologies of its body and wings are based on the Hawkmoth *Manduca sexta* by referring to the studies of O'Hara et al [1] and Ellington [2]. The wings are assumed to be massless and rigid. In addition, aerodynamic effects on the body are ignored.

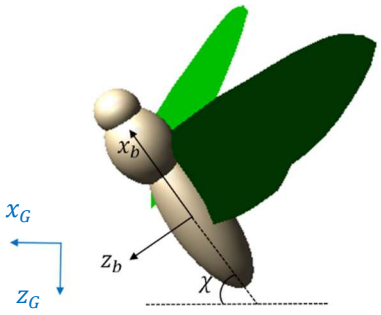

Figure 1 - FWMAV(Manduca sexta)model.

Figure 1 shows FWMAV model used in this study. The body-fixed coordinate whose origin located at the center of mass of body is expressed by using subscript b. Global coordinate is expressed by subscript G. Body pitch angle written as χ means the angle between the body-fixed coordinate and the global coordinate.

2.2 Definition of wing kinematics

The wing kinematics are described using three angles, stroke position angle (ϕ), feathering angle(α)and deviation angle(θ). Each rotational angle is set as follows:

*contact email: jaehunghan@kaist.edu

$$\phi(t) = \phi_0 - \phi_{amp}\sin(2\pi ft)$$
$$\alpha(t) = \alpha_0 - \frac{\alpha_{amp}}{\tanh(C_\alpha)}\tanh(C_\alpha\cos(2\pi ft)) \quad (1)$$
$$\theta(t) = 0$$

2.3 Aerodynamic model

To describe the aerodynamic load on the flapping wing, the semi-empirical quasi-steady aerodynamic model from the study of Han et al. [3] is used. This model compensates the influence of the advance ratio J by defining aerodynamic coefficients as functions of the angle of attack and advance ratio J both. These coefficients (Equation 2) were obtained by conducting 147 individual experiment cases at each advance ratio J value and angle of attack value. For more details, refer to Han et al.[3]

$$\begin{aligned} C_L(\alpha,J) &= K_{p,L}(J)\sin(\alpha)\cos^2(\alpha) \\ &\quad + K_{V,L}(J)\sin^2(\alpha)\cos(\alpha) \\ C_D(\alpha,J) &= K_{P,D}(J)\sin^2(\alpha)\cos(\alpha) \\ &\quad + K_{V,D}(J)\sin^3(\alpha) \\ C_M(\alpha,J) &= K_{P,M}(J)\sin^2(\alpha)\cos(\alpha) \\ &\quad + K_{V,M}(J)\sin^2(\alpha) \end{aligned} \quad (2)$$

$$J = \frac{U_\infty}{U_{tip}} = \frac{u_G}{4\phi_{amp}Rf} \quad (3)$$

The advance ratio is defined as the ratio of forward flight speed to mean wing tip velocity as shown in Equation 3.

2.4 Equation of motion and linearization

Equation 4 is the 3-DOF longitudinal equations of motion expressed in body-fixed coordinate. Here, the X , Z and M are periodic aerodynamic forces and moment induced by wing motion. u , w and q are the velocities of x and z direction of the body-fixed coordinate and the body pitch rate, respectively.

$$\begin{aligned} X - mg\sin\chi &= m(\dot{u} + qw) \\ Z + mg\cos\chi &= m(\dot{w} - qu) \\ M &= I_{yy}\dot{q} \end{aligned} \quad (4)$$

Equation 4 can be linearized around equilibrium points using the cycle-average method and the small perturbation theory. Equation 5 is the linearized equation of motion expressed in matrix form.

$$\begin{bmatrix} \Delta\dot{\bar{u}} \\ \Delta\dot{\bar{w}} \\ \Delta\dot{\bar{q}} \\ \Delta q \end{bmatrix} = \begin{bmatrix} \frac{\bar{X}_{\bar{u}}}{m} & \frac{\bar{X}_{\bar{w}}}{m} & \frac{\bar{X}_{\bar{q}}}{m} - \bar{U}_\infty\sin\chi & -g\cos\chi \\ \frac{\bar{Z}_{\bar{u}}}{m} & \frac{\bar{Z}_{\bar{w}}}{m} & \frac{\bar{Z}_{\bar{q}}}{m} + \bar{U}_\infty\cos\chi & -g\sin\chi \\ \frac{\bar{M}_{\bar{u}}}{I_{yy}} & \frac{\bar{M}_{\bar{w}}}{I_{yy}} & \frac{\bar{M}_{\bar{q}}}{I_{yy}} & 0 \\ 0 & 0 & 1 & 0 \end{bmatrix} \begin{bmatrix} \Delta\bar{u} \\ \Delta\bar{w} \\ \Delta q \\ \Delta\bar{\Theta} \end{bmatrix} \quad (5)$$

More details on process and the assumption of the linearization can be found in the study of Kim et al. [4].

2.5 Trim search

Since the linearization of nonlinear system is conducted near equilibrium points, equilibrium points should be found first. To find out the trim conditions, which make the FWMAV model slightly oscillate around an equilibrium point, we employed the gradient-based trim search algorithm from the study of Kim et al. [4]. This trim search algorithm runs the dynamic simulation of FWMAV during the one flapping period iteratively as changing the initial conditions until the mean velocity and excessive force and moment conditions are satisfied. The excessive forces and moment are compensated by using inverse matrix of control effective matrix B that consists of the partial derivative of force and moment to each control parameters. The control effective matrix B contains gradient information of the aerodynamic force and moment with respect to each control parameters. In this study,

wing stroke frequency (f), mean stroke angle (ϕ_0) and mean feathering angle(α_0) were chosen as control parameters. The more precise and detailed expression and procedure can be referred to Kim et al. [4]. For dynamic simulation, the ode45 solver with 10^{-4} time step size in MATLAB® Simulink was used.

$$B = \begin{bmatrix} \frac{\partial \overline{X_G}}{\partial f} & \frac{\partial \overline{X_G}}{\partial \phi_0} & \frac{\partial \overline{X_G}}{\partial \alpha_0} \\ \frac{\partial \overline{Z_G}}{\partial f} & \frac{\partial \overline{Z_G}}{\partial \phi_0} & \frac{\partial \overline{Z_G}}{\partial \alpha_0} \\ \frac{\partial \overline{M}}{\partial f} & \frac{\partial \overline{M}}{\partial \phi_0} & \frac{\partial \overline{M}}{\partial \alpha_0} \end{bmatrix} \quad (6)$$

To find the trim condition at each forward speed, the reference body pitch angle should be determined as a function of forward speed. Since it was well known that body of FWMAV tilts more toward forward flight direction as it moves faster, which means χ decreases as speed increases from the study of [5], we determined the body pitch angle at each forward flight speed as simple linear function as described in Equation 7. The body pitch angle is 70 degree at hovering state and decreases linearly at rate of $20\,\mathrm{deg}/\,(m/s)$.

$$\chi(\mathrm{deg}) = 70 - 20u_G \quad (7)$$

2.6 Optimal control gain matrices decision with LQR method.

At each trim condition, the linearized equations of motion with control effectiveness matrix B are obtained.

$$\begin{bmatrix} \Delta\dot{\bar{u}} \\ \Delta\dot{\bar{w}} \\ \Delta\dot{\bar{q}} \\ \Delta q \end{bmatrix} = A \begin{bmatrix} \Delta\bar{u} \\ \Delta\bar{w} \\ \Delta\bar{q} \\ \Delta\bar{\chi} \end{bmatrix} + B_u \begin{bmatrix} \Delta f \\ \Delta\phi_0 \\ \Delta\alpha_0 \end{bmatrix} \quad (8)$$

The detail terms for the matrix A can be found in Equation 5. B_u is the body-fixed coordinate and the normalized version of B is given in Equation 6.

$$B_u = \begin{bmatrix} \frac{\partial \overline{X_b}}{\partial f}/m & \frac{\partial \overline{X_b}}{\partial \phi_0}/m & \frac{\partial \overline{X_b}}{\partial \alpha_0}/m \\ \frac{\partial \overline{Z_b}}{\partial f}/m & \frac{\partial \overline{Z_b}}{\partial \phi_0}/m & \frac{\partial \overline{Z_b}}{\partial \alpha_0}/m \\ \frac{\partial \overline{M_b}}{\partial f}/I_{yy} & \frac{\partial \overline{M_b}}{\partial \phi_0}/I_{yy} & \frac{\partial \overline{M_b}}{\partial \alpha_0}/I_{yy} \\ 0 & 0 & 0 \end{bmatrix} \quad (9)$$

Since the uncertainties in dynamic modelling can make an offset, we set an integral state (Equation 10) to obtain the augmented equation (Equations 11 and 12).

$$X_I = \int_{t_{start\ of\ cycle}}^{t_{end\ of\ cycle}} y\, d\tau \quad (10)$$

$$\begin{bmatrix} \dot{X} \\ \dot{X}_I \end{bmatrix} = \begin{bmatrix} A & 0 \\ C & 0 \end{bmatrix} \begin{bmatrix} X \\ X_I \end{bmatrix} + \begin{bmatrix} B \\ 0 \end{bmatrix} u \quad (11)$$

$$\widetilde{\dot{X}} = \widetilde{A}\widetilde{X} + \widetilde{B}u \quad (12)$$

Here, C matrix is defined as

$$C = \begin{bmatrix} \cos\chi_{ref} & \sin\chi_{ref} & 0 & 0 \\ -\sin\chi_{ref} & \cos\chi_{ref} & 0 & -U_\infty \\ 0 & 0 & 0 & 1 \end{bmatrix} \quad (13)$$

By using the augmented version of the equation (Equation 12) and the weight matrices(R and Q), we could obtain the optimal gain matrix $\widetilde{K}$. R is the weight matrix for the control input parameters and Q is the weight matrix for the states.

$$R = \begin{bmatrix} 100 & & \\ & 100 & \\ & & 100 \end{bmatrix} \quad (14)$$

$$Q = \begin{bmatrix} 1 & & & & & & \\ & 1 & & & & & \\ & & 10^{-4} & & & & \\ & & & 0.01 & & & \\ & & & & 10 & & \\ & & & & & 10 & \\ & & & & & & 20 \end{bmatrix} \quad (15)$$

$\widetilde{K}$ can be divided into two parts, one is for the original states and the other is for the integral states.

$$\widetilde{K} = [K \; K_I] \quad (16)$$

$$u = -KX - \sum K_{I,i} X_{I,i} \quad (17)$$

Equation 17 shows how the control input u is determined for the next cycle. Here, since the control input is updated at every half period and the control gain matrix changes with the reference velocity, the integral state parts of Equation 17 is accumulated whenever the control gain is updated, instead of being calculated by multiplying $K_{I,i}$ to an integrated value over whole simulation time.

3 RESULT AND DISCUSSION

3.1 Trim search results

Figure 2 shows the trimmed wing kinematics results at each flight speed. The flapping frequency decreases overall as flight speed increases. On the other hand, the mean stroke angle and the mean feathering angle increase as the flight speed decreases. Increased mean stroke angle means that mid stroke line goes back with respect to the body. Increased mean feathering angle represents increased angle of attack at downstroke and decreased angle of attack at upstroke. This combinations of wing kinematic control parameters at each flight speed generate proper forces and moment to stay in trim condition. The gain matrix $\widetilde{K}$ is also obtained at each trim condition. Figure 3 and 4 show the components of K and K_I in Equation 16, respectively. The gain matrix $\widetilde{K}$ is set as functions of forward flight speed from the trim condition results by linearly interpolating between two nearest point.

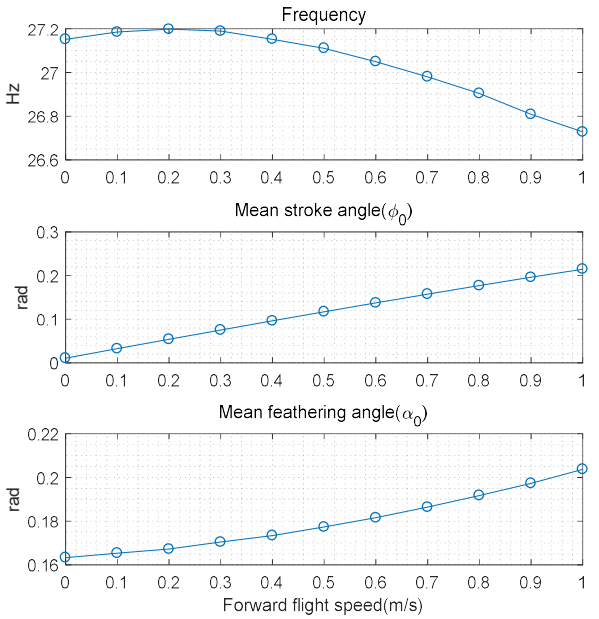

Figure 2 Trimmed wing kinematic parameters

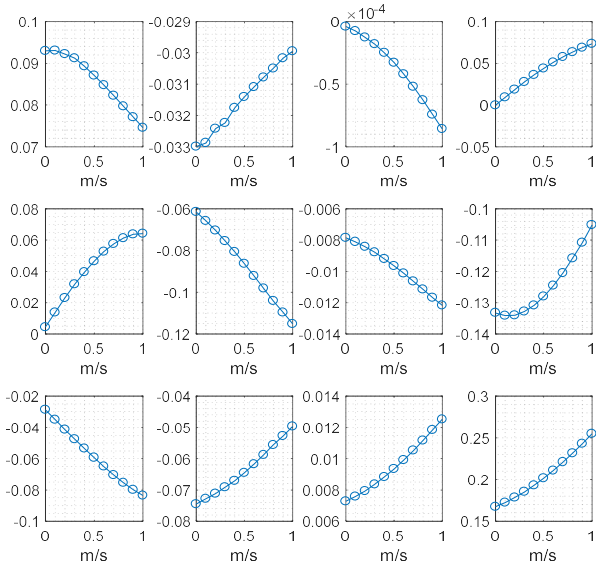

Figure 3 Component values of matrix K respect to flight speed

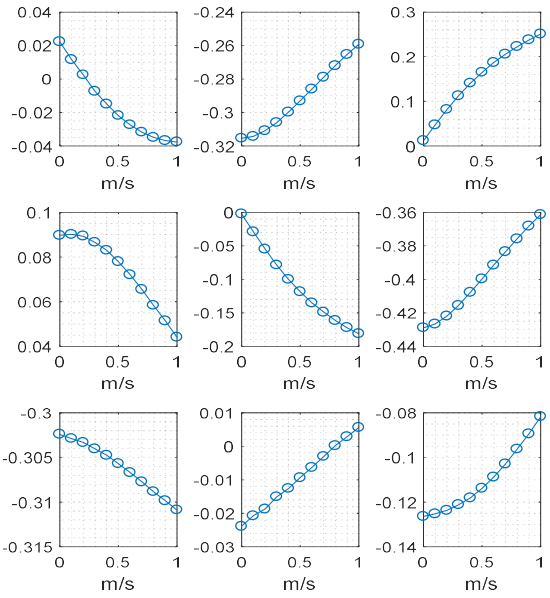

Figure 4 Component values of matrix K_I respect to flight speed

3.2 Flight control for varying reference velocity.

To see whether the designed gain-scheduled controller works well, the control simulation for the varying reference velocity was conducted. The reference velocity varies between 0m/s and 1m/s. Upper plot of Figure 6 Shows the velocity results. The red and blue lines represent the horizontal velocity reference and the horizontal velocity of FWMAV, respectively. The purple and yellow lines represent the vertical velocity reference and the vertical velocity of the FWMAV. The velocity results show that the model with controller follows the horizontal velocity reference well and the vertical velocity of model stays around 0m/s. The body pitch angle also follows the reference. There is a little deviation between the reference and body pitch angle of model during accelerating and decelerating. It seems that unwanted effects of accelerating and decelerating make the body pitch angle slightly deviated from the reference. Figure 5 shows the changes of the control parameters during the flight control simulation. The control parameters are changed in reasonably small range.

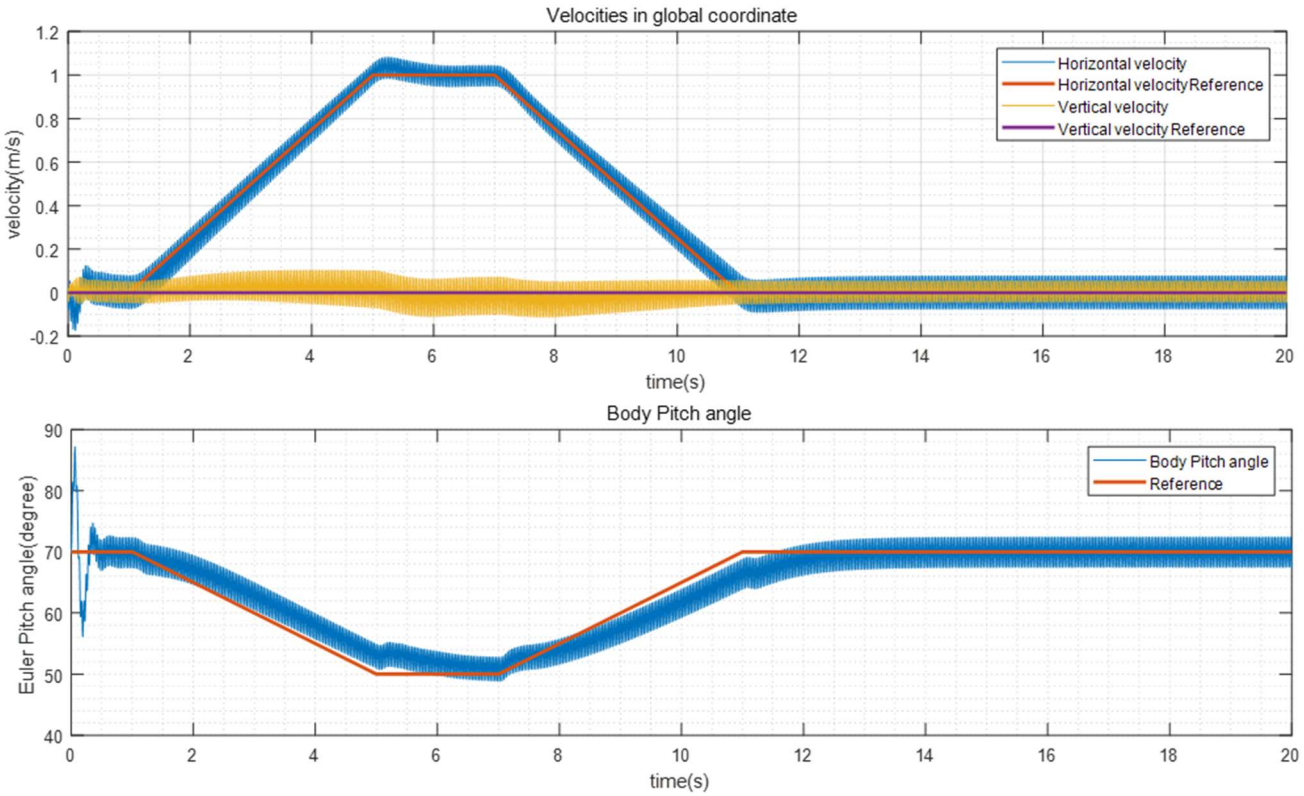

Figure 5 Control parameters during the flight control simulation

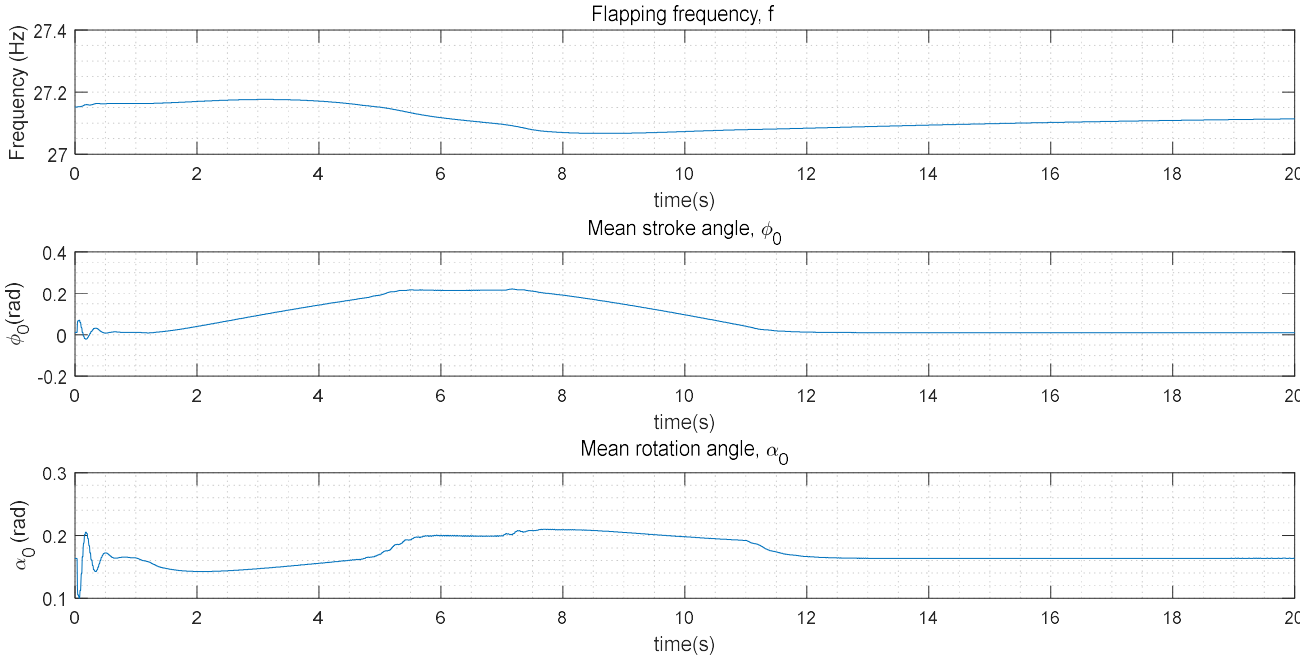

Figure 6 Flight control simulation results for varying reference velocity.

4 CONCLUSION

In this study, the forward flight control simulation of FWMAV is conducted. The equation of motion for a FWMAV is obtained using a semi empirical aerodynamic model and a rigid body dynamics approach. The control of FWMAV using wing kinematics variations is studied. It is shown that the designed gain scheduled controller works well for the speed tracking problems.

ACKNOWLEDGEMENTS

This research was supported by Basic Science Research Program through the National Research Foundation of Korea (NRF) funded by the Ministry of Science, ICT & Future Planning (NRF-2017R1A2B4005676).

REFERENCES

[1] R.P. O'Hara, N. Deleon, and A. Palazotto. Structural identification and simulation of a MAV forewing. Composite Structures, 119, 315-321, 2015.

[2] C.P. Ellington. The Aerodynamics of Hovering Insect Flight. II. Morphological Parameters. Philosophical Transactions of the Royal Society of London. Series B, Biological Sciences, 305(1122): 17–40, 1984.

[3] J.-S. Han, J. Chang, J.-H Han, Jae-Hung. An aerodynamic model for insect flapping wings in forward flight. Bioinspiration & biomimetics, 12(3) : 036004 2017.

[4] J.K. Kim, J. S. Han, J. S. Lee, and J. H. Han Hovering and forward flight of the hawkmoth Manduca sexta: trim search and 6-DOF dynamic stability characterization. Bioinspiration & biomimetics, 10(5): 056012, 2015.

[5] C.P. Ellington. The Aerodynamics of Hovering Insect Flight. III. Kinematics. Philosophical Transactions of the Royal Society of London. Series B, Biological Sciences, 305(1122): 41–78, 1984.